Electronic Supplementary Information

Halo-methylphenyl substituted neutral tripodal receptors for cation-asisted encapsulation of anionic guests of varied dimensionality

Utsab Manna and Gopal Das*

Department of Chemistry, Indian Institute of Technology Guwahati,

Assam-781039, India

E-mail: gdas@iitg.ernet.in

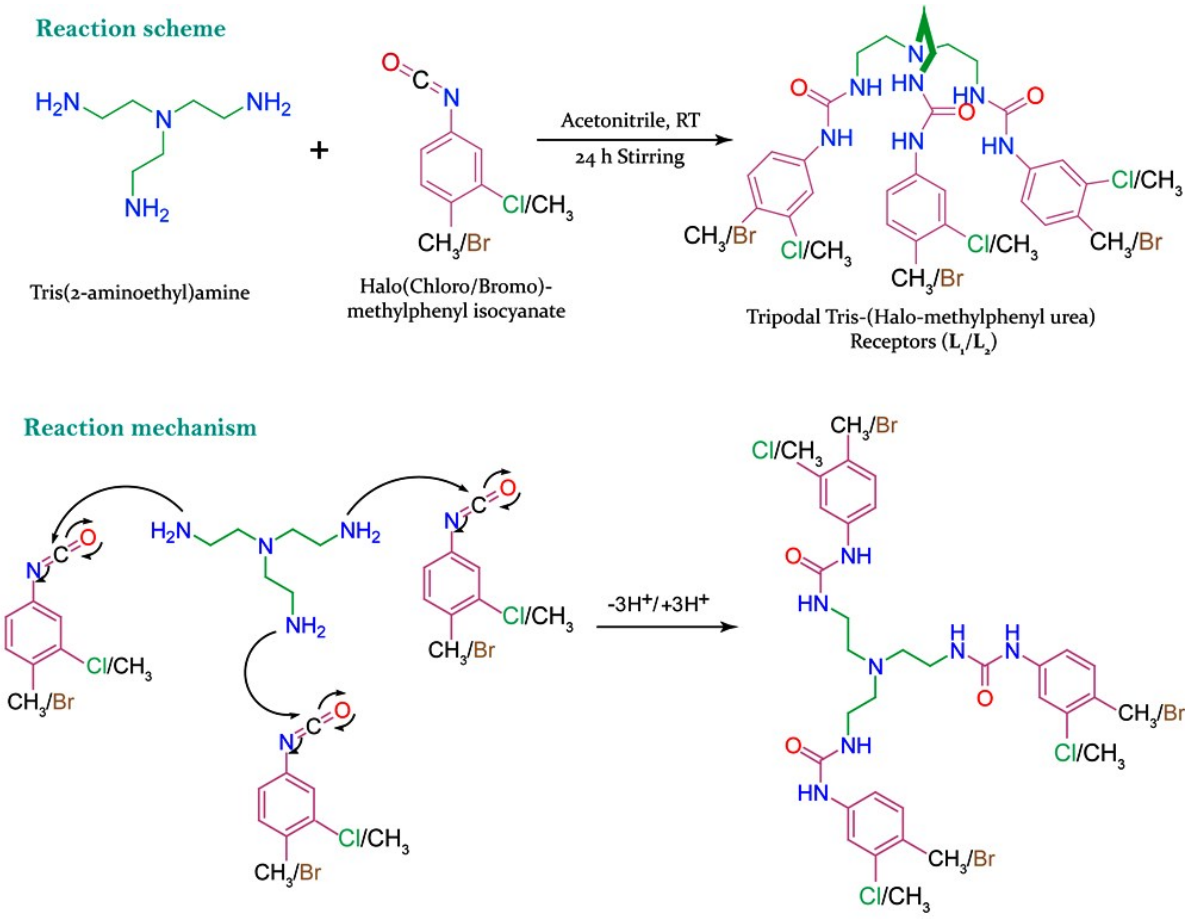

Scheme S1: Synthetic pathway and reaction mechanism for preparation of two isomeric halo-methylphenyl tris-urea receptors $\mathbf{L_1}$ and $\mathbf{L_2}$.

Characterization of free receptors L_1 and L_2:

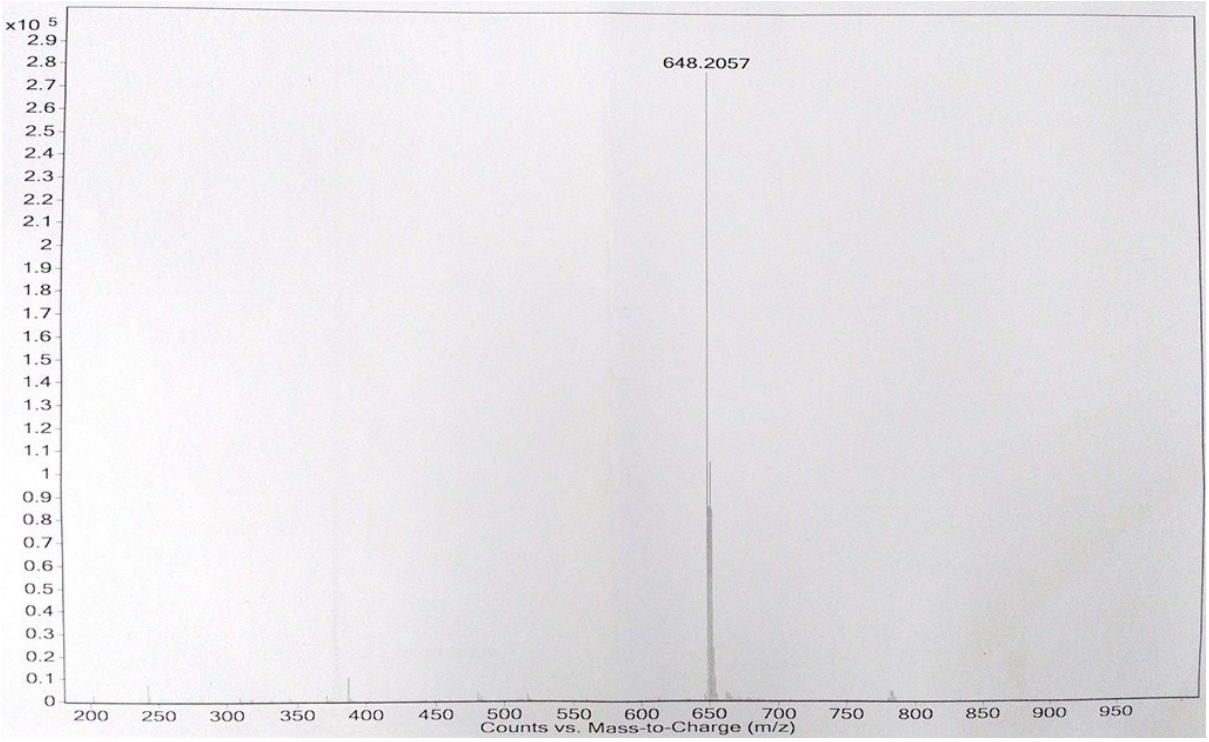

Figure S1: ESI-mass spectrum of tris([(3-chloro-4-methylphenyl)amino]ethyl)-urea receptor **L_1.**

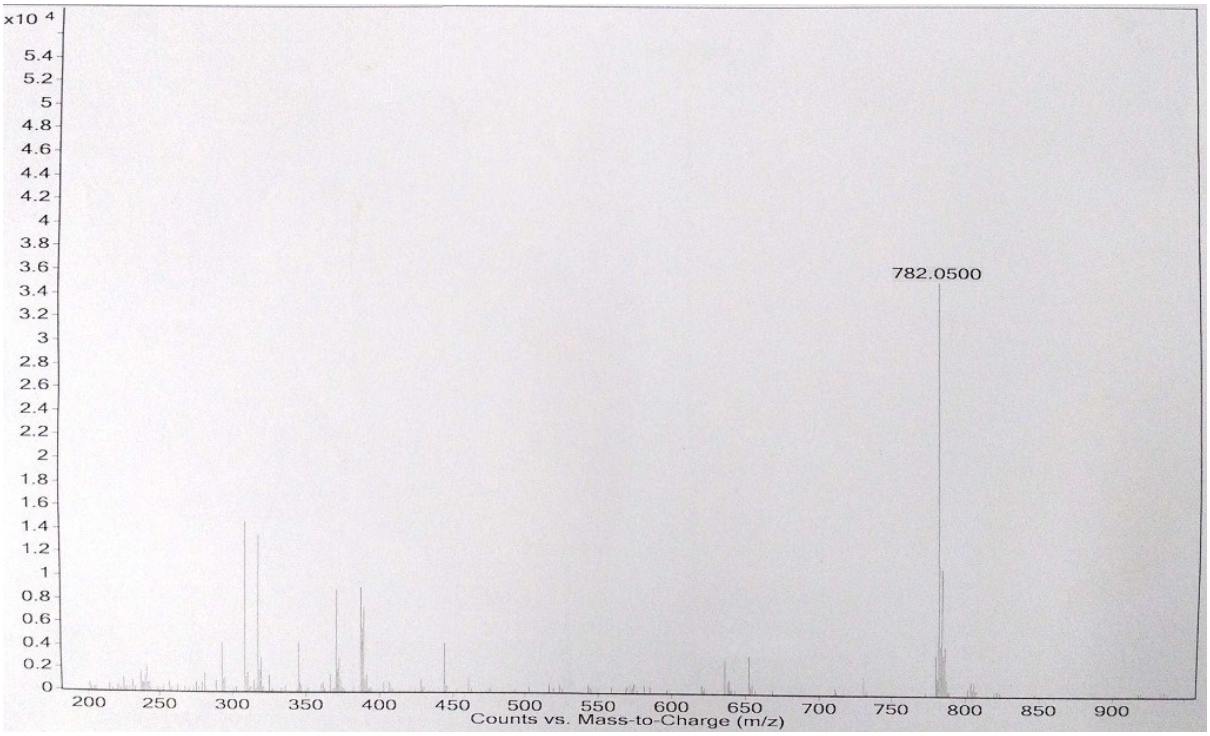

Figure S2: ESI-mass spectrum of tris([(4-Bromo-3-methylphenyl)amino]ethyl)-urea receptor **L_2.**

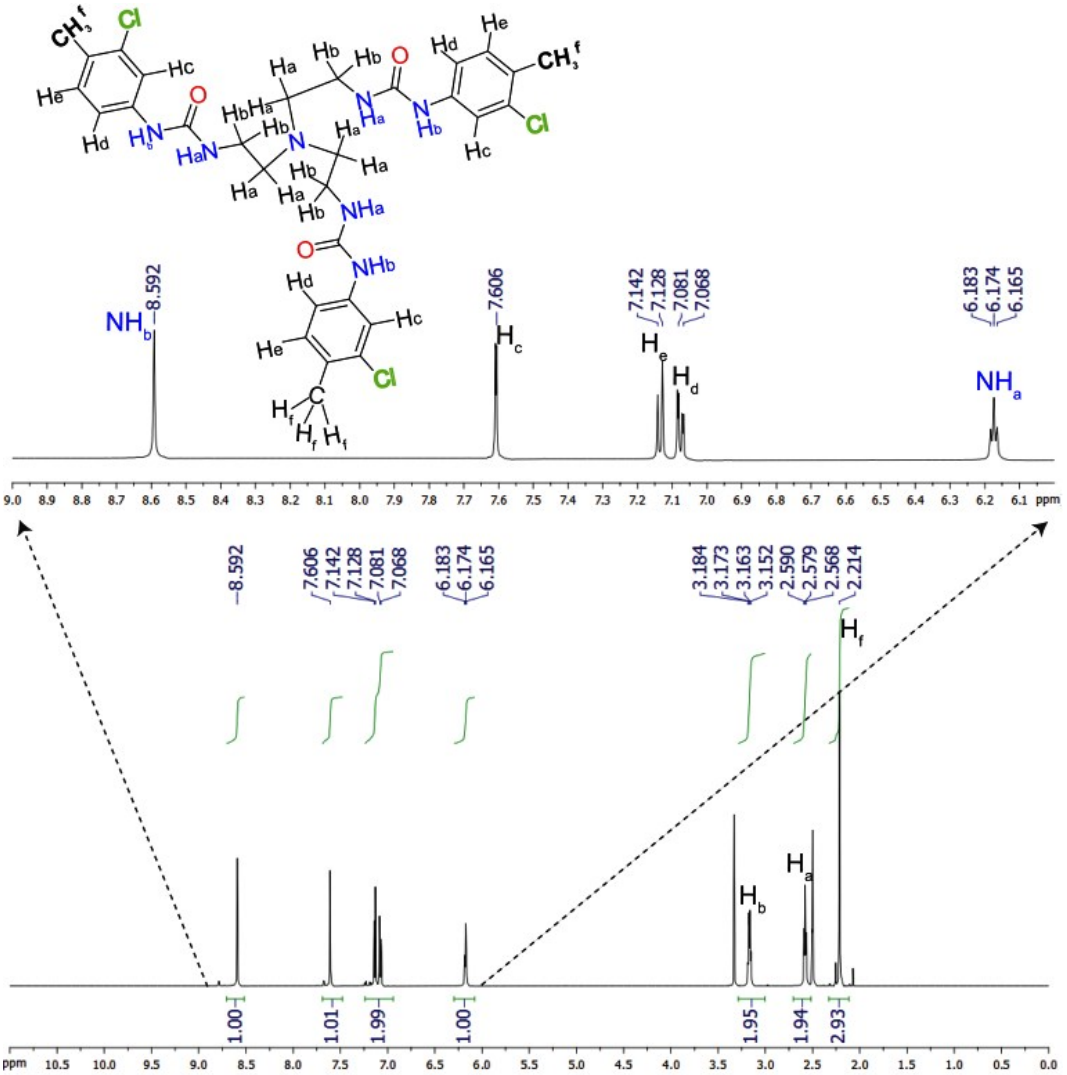

Figure S3: Integrated ^{1}H-NMR spectrum (full as well as expanded) and interpretation of all hydrogen atoms of free tripodal tris-urea receptor $\mathbf{L_1}$ in DMSO-d_6 at 25ºC.

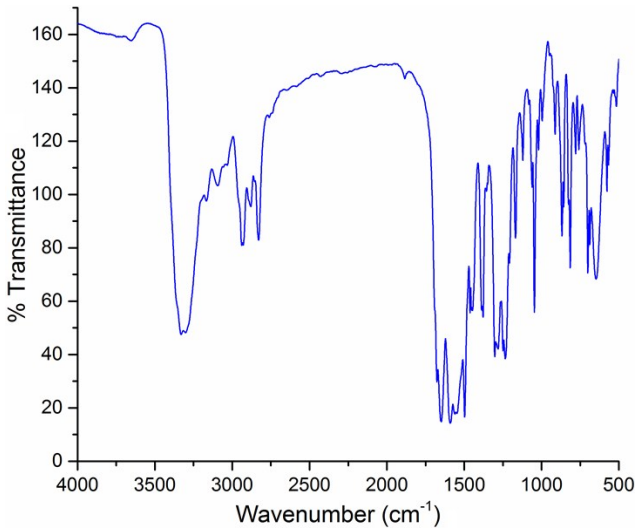

Figure S4: FT-IR spectrum of Free ligand $\mathbf{L_1}$ recorded in KBr pellet.

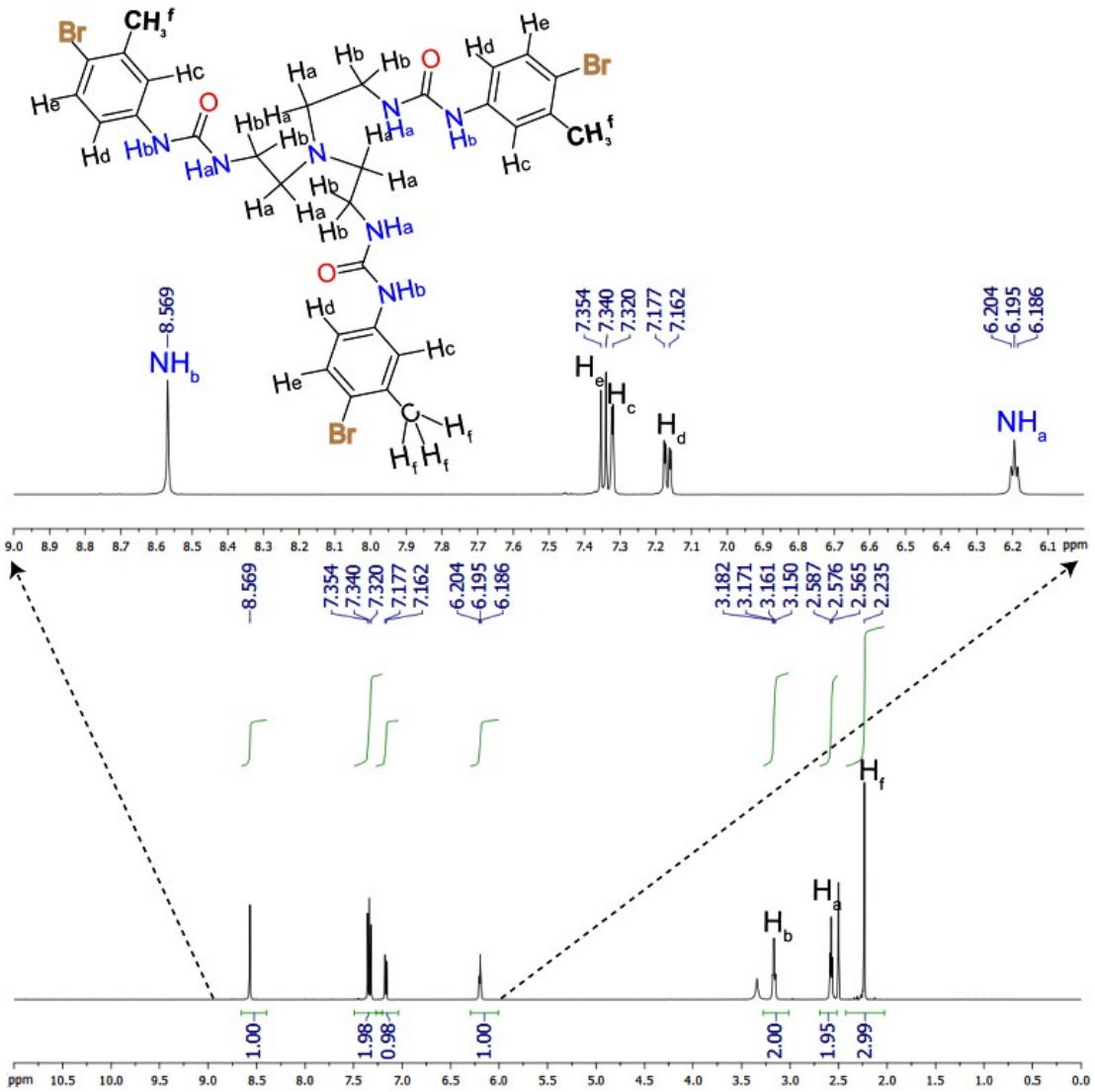

Figure S5: Integrated ^{1}H-NMR spectrum (full as well as expanded) and interpretation of all hydrogen atoms of free tripodal tris-urea receptor $\mathbf{L_2}$ in DMSO-d_6 at 25ºC.

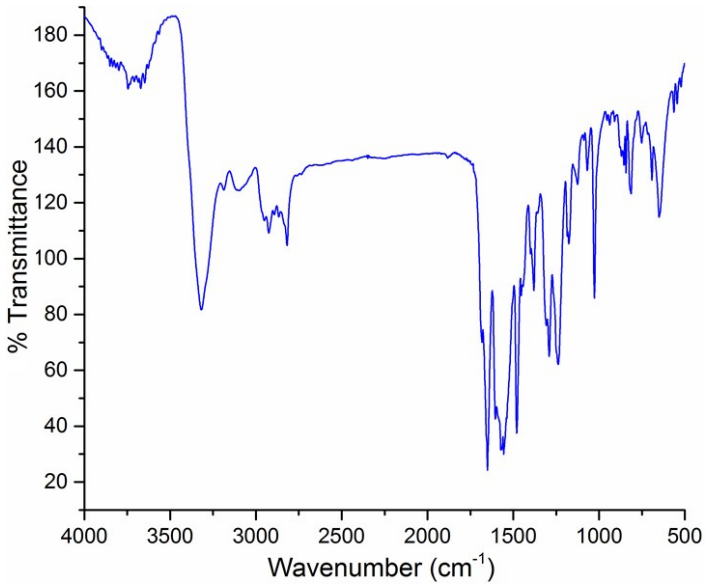

Figure S6: FT-IR spectrum of Free ligand $\mathbf{L_1}$ recorded in KBr pellet.

Characterization of anion complexes of receptors:

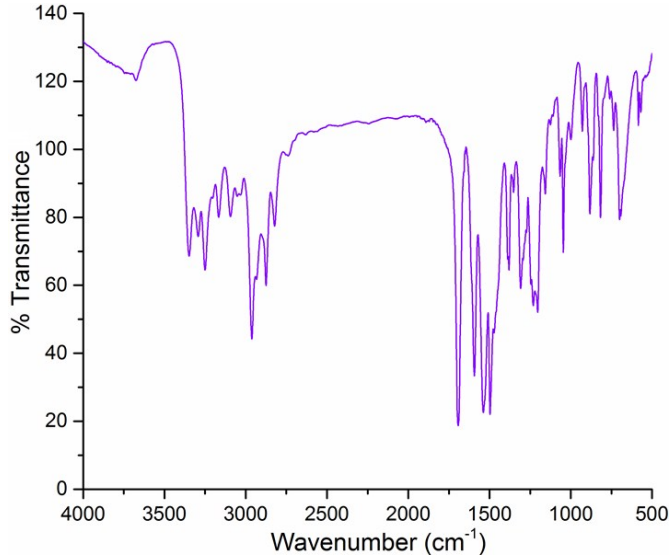

Figure S7: FT-IR spectrum of chloride encapsulated complex **1a** of $\mathbf{L_1}$ recorded in KBr pellet.

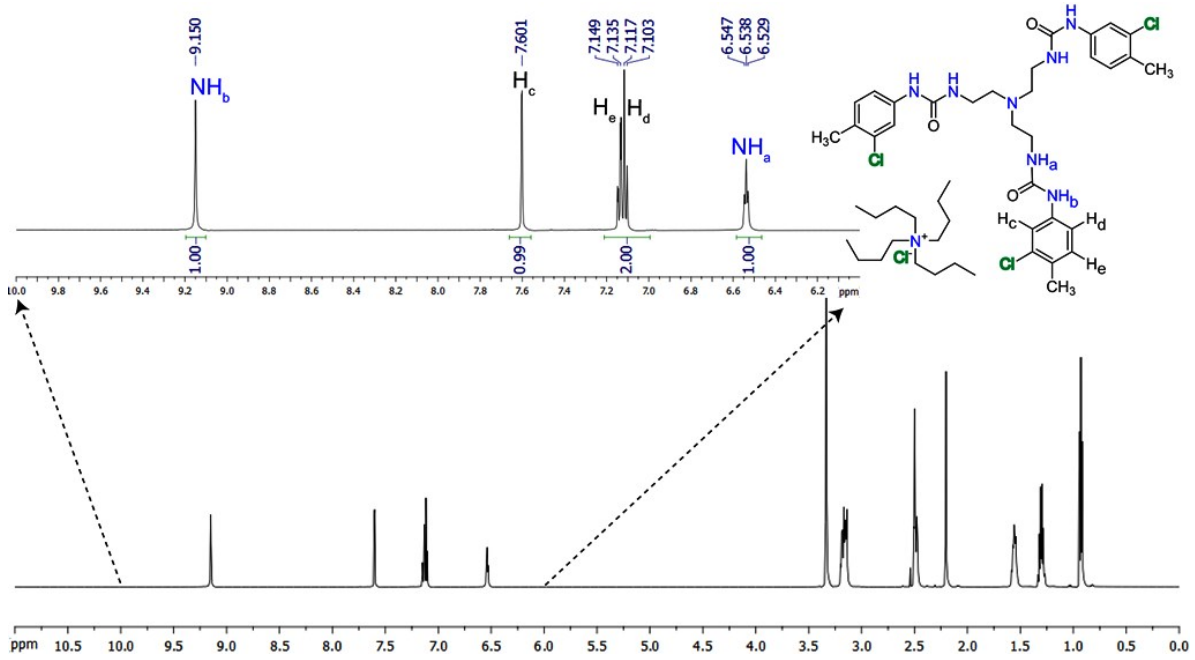

Figure S8: ^{1}H NMR full and expanded spectrum of chloride encapsulated complex **1a** as recorded in DMSO-d_6 at 298 K.

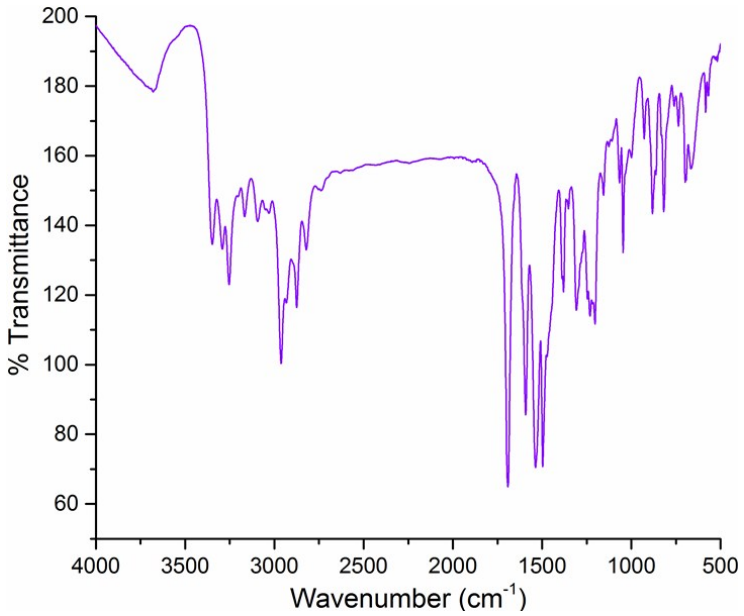

Figure S9: FT-IR spectrum of bromide encapsulated complex **1b** of $\mathbf{L_1}$ recorded in KBr pellet.

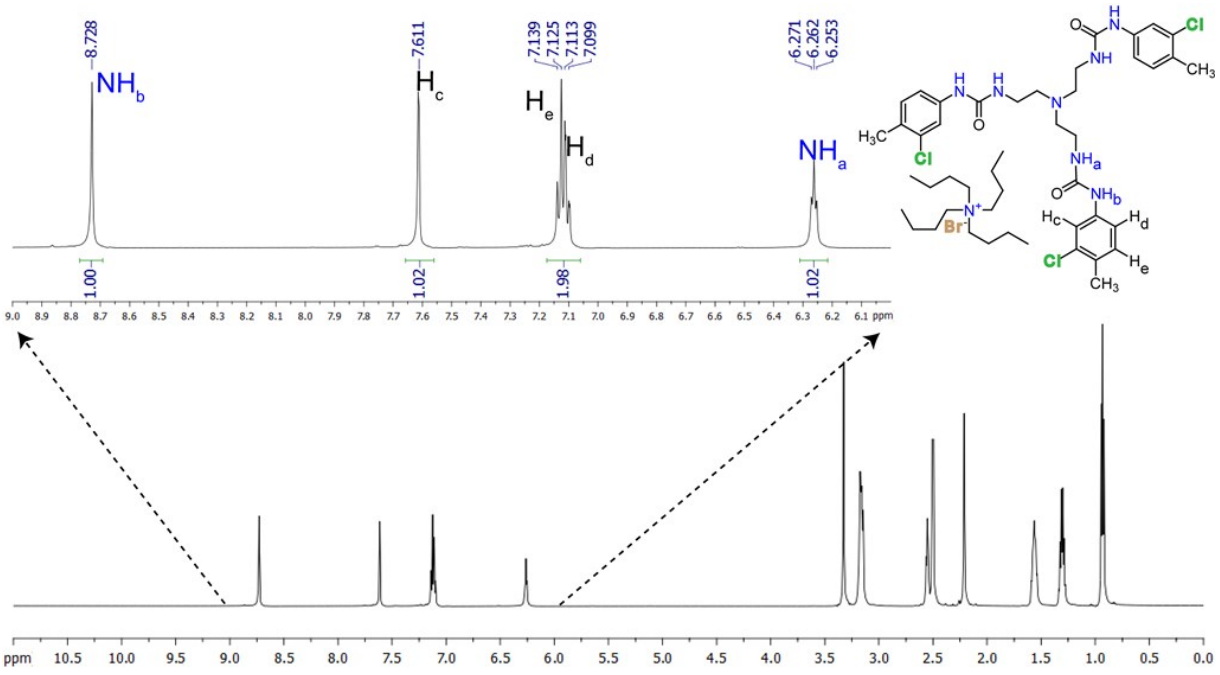

Figure S10: ^{1}H NMR full and expanded spectrum of bromide encapsulated complex **1b** as recorded in DMSO-d_6 at 298 K.

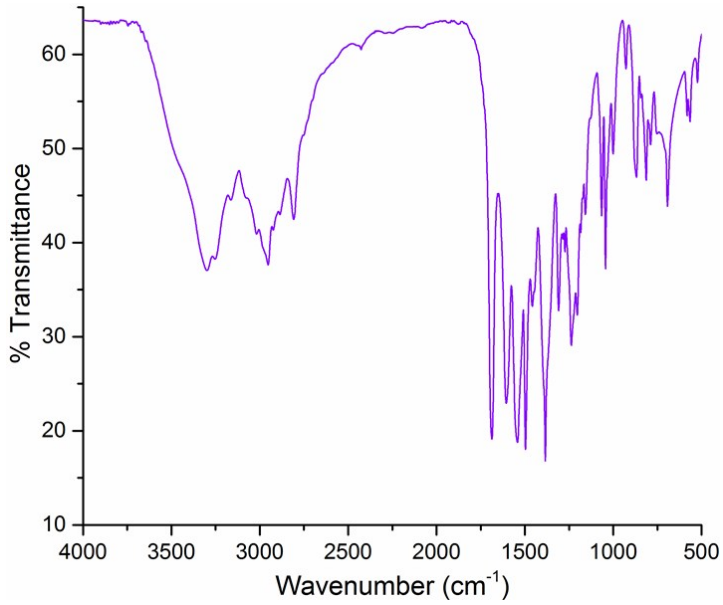

Figure S11: FT-IR spectrum of divalent carbonate encapsulated complex **1c** of $\mathbf{L_1}$ recorded in KBr pellet.

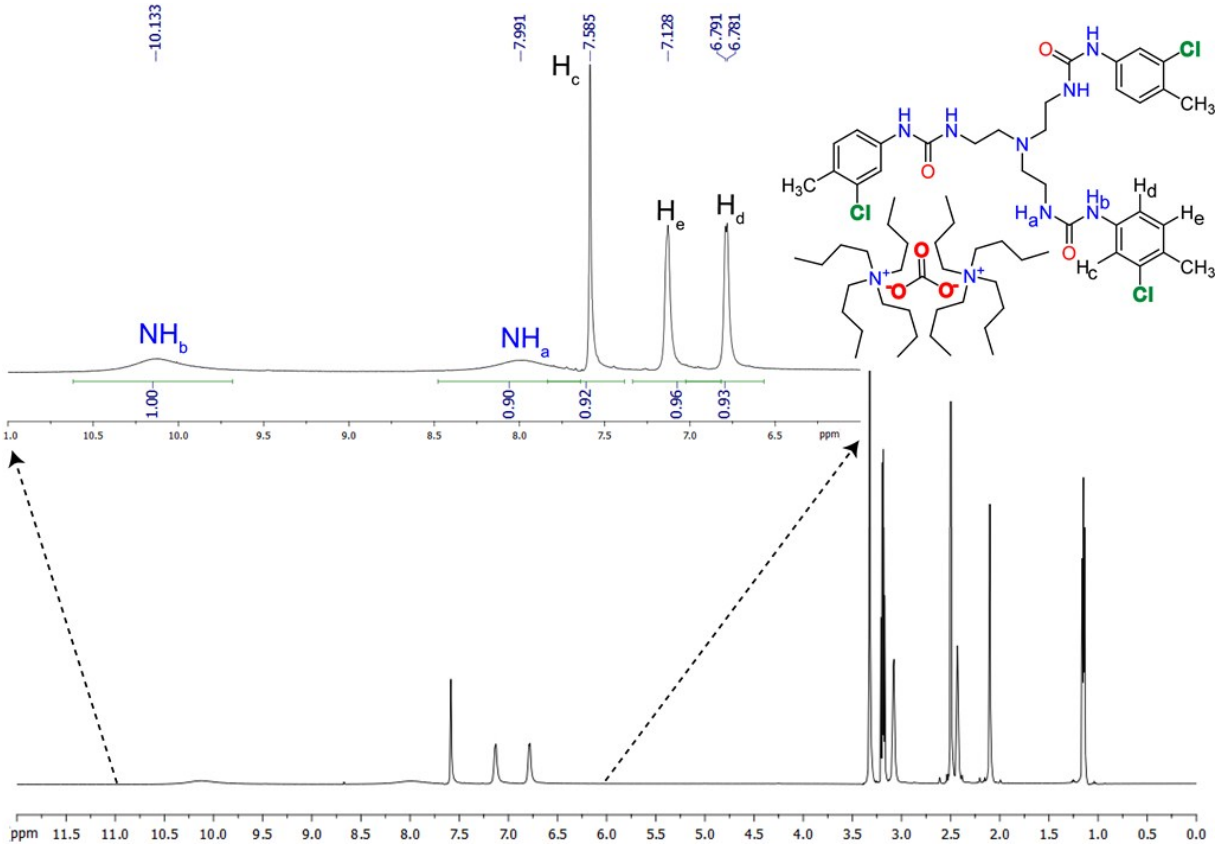

Figure S12: ^{1}H NMR full and expanded spectrum of divalent carbonate encapsulated dimeric cage complex **1c** as recorded in DMSO-d_6 at 298 K.

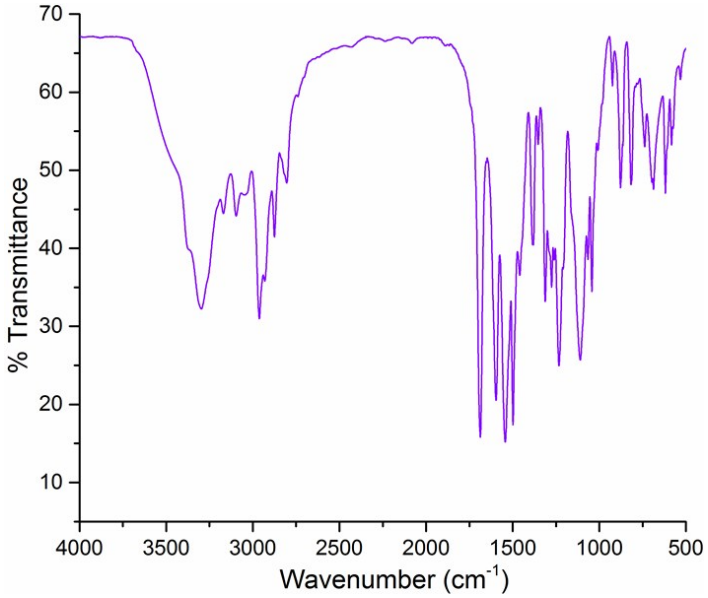

Figure S13: FT-IR spectrum of divalent sulphate encapsulated complex **1d** of $\mathbf{L_1}$ recorded in KBr pellet.

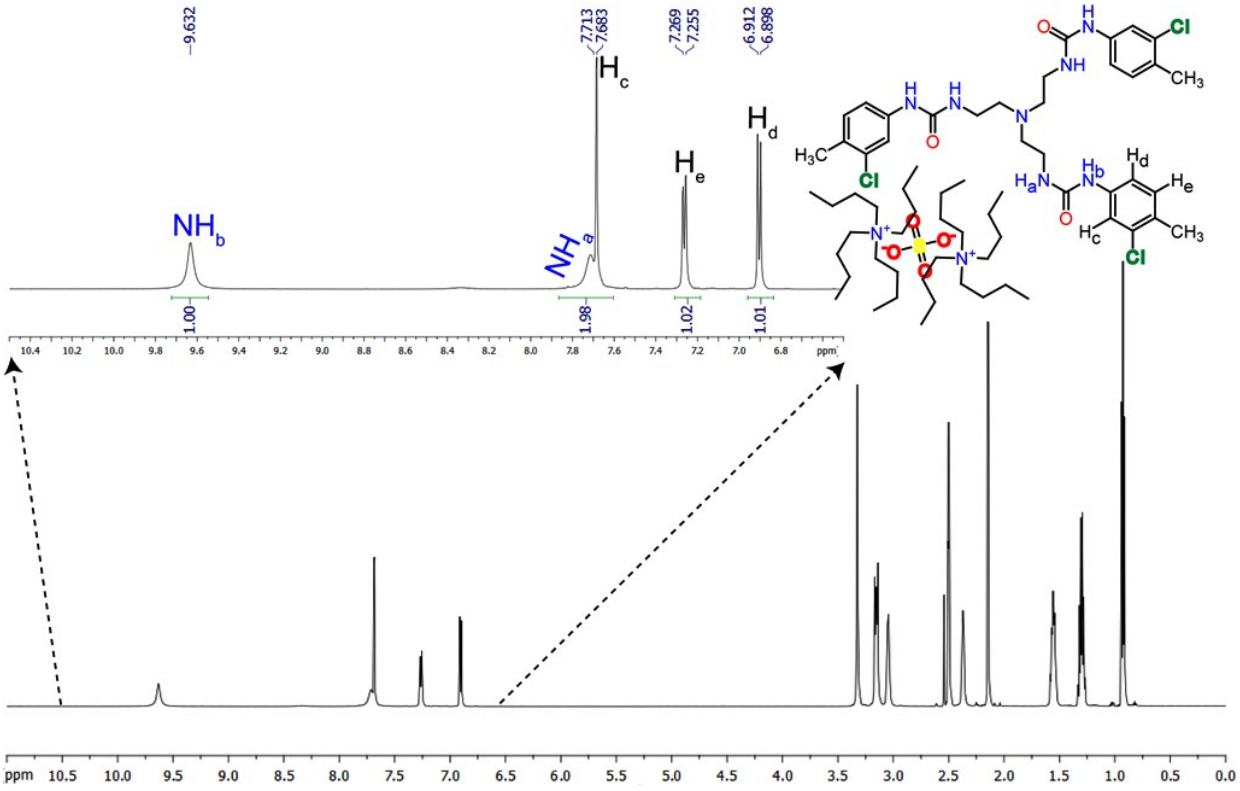

Figure S14: ^{1}H NMR full and expanded spectrum of divalent sulphate encapsulated dimeric cage complex **1d** as recorded in DMSO-d_6 at 298 K.

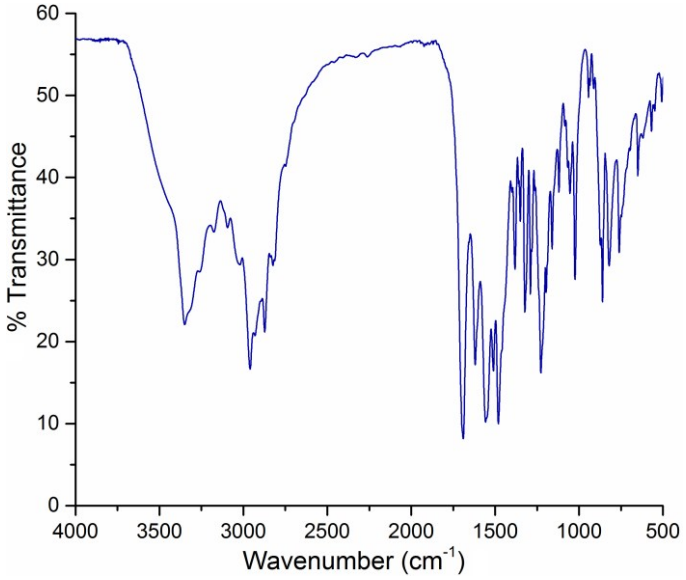

Figure S15: FT-IR spectrum of fluoride encapsulated complex **2a** of $\mathbf{L_2}$ recorded in KBr pellet.

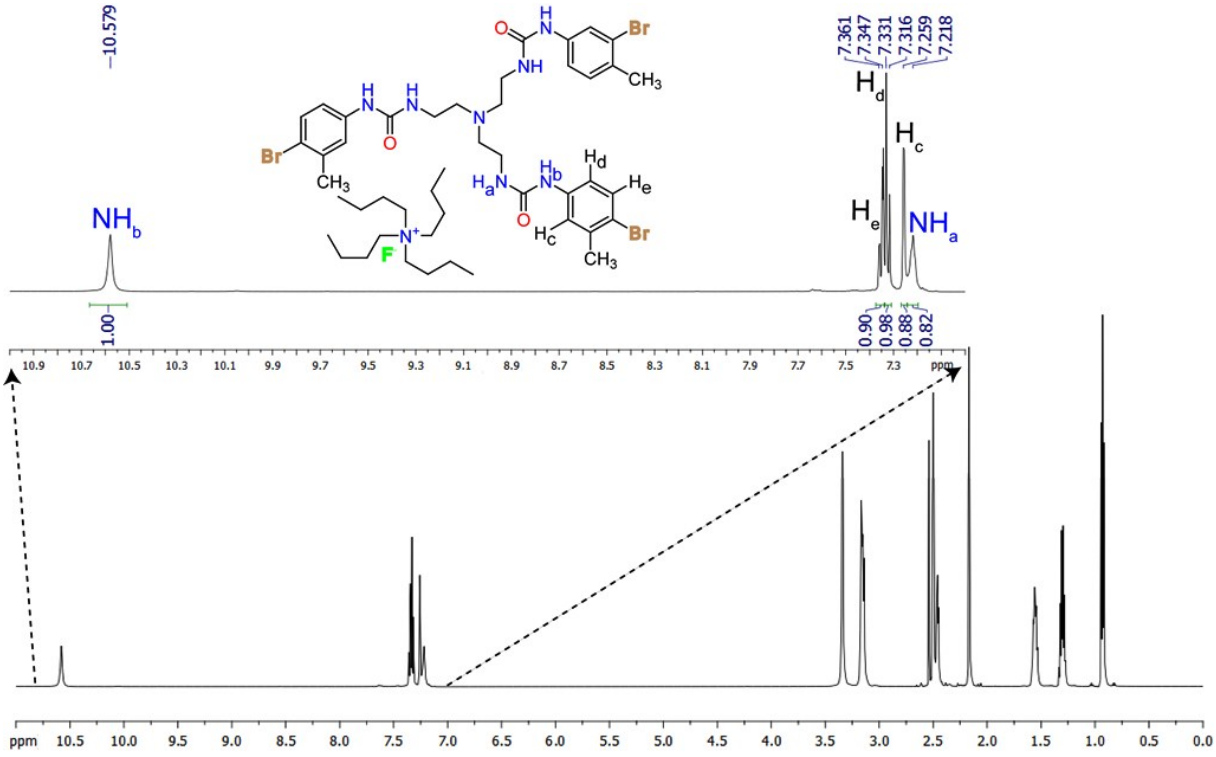

Figure S16: ^{1}H NMR full and expanded spectrum of fluoride encapsulated complex **2a** as recorded in DMSO-d_6 at 298 K.

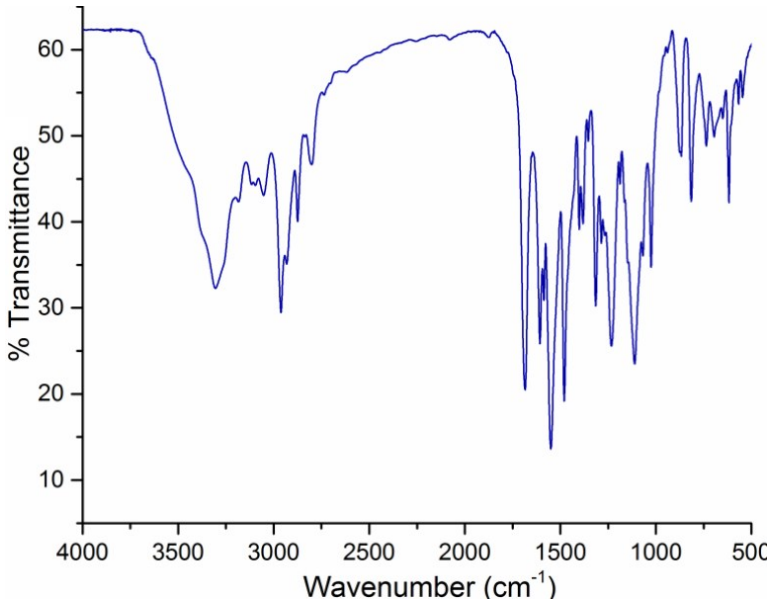

Figure S17: FT-IR spectrum of divalent sulphate encapsulated complex **2b** of $\mathbf{L_2}$ recorded in KBr pellet.

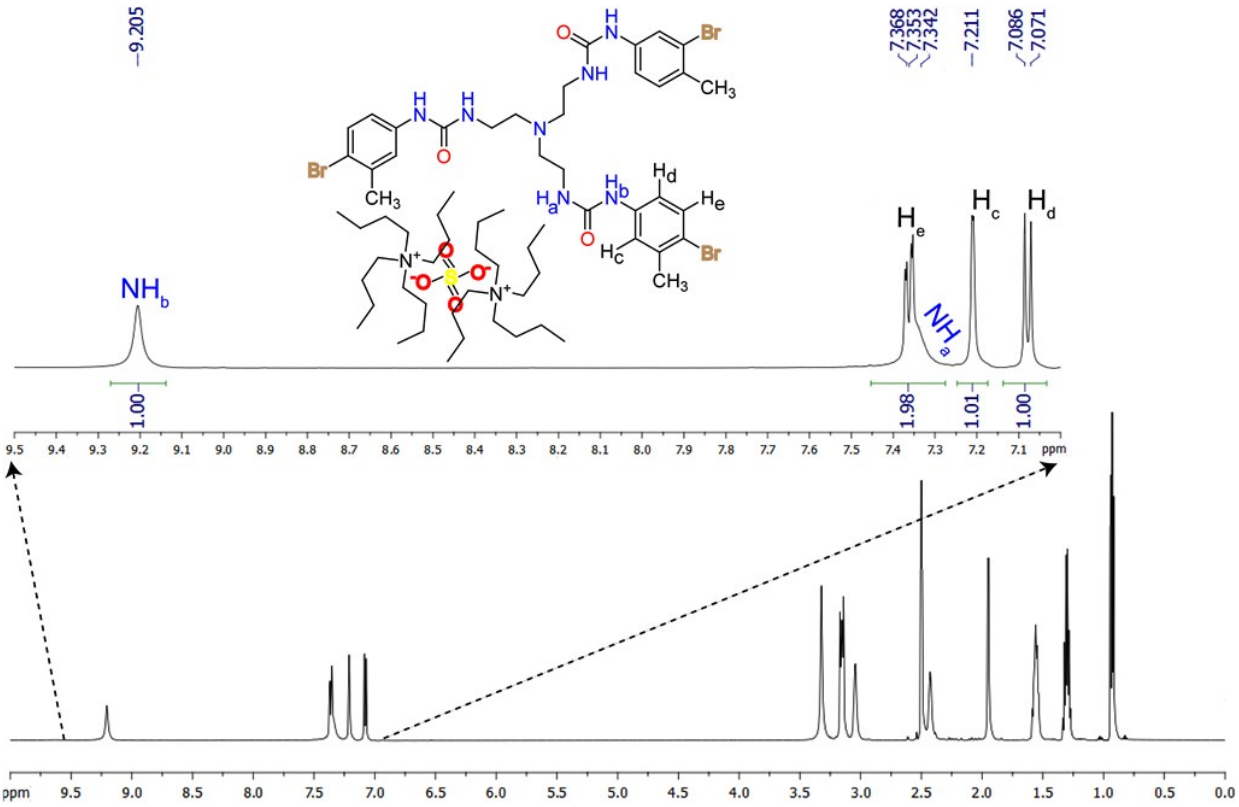

Figure S18: ^{1}H NMR full and expanded spectrum of divalent sulphate encapsulated dimeric cage complex **2b** as recorded in DMSO-d_6 at 298 K.

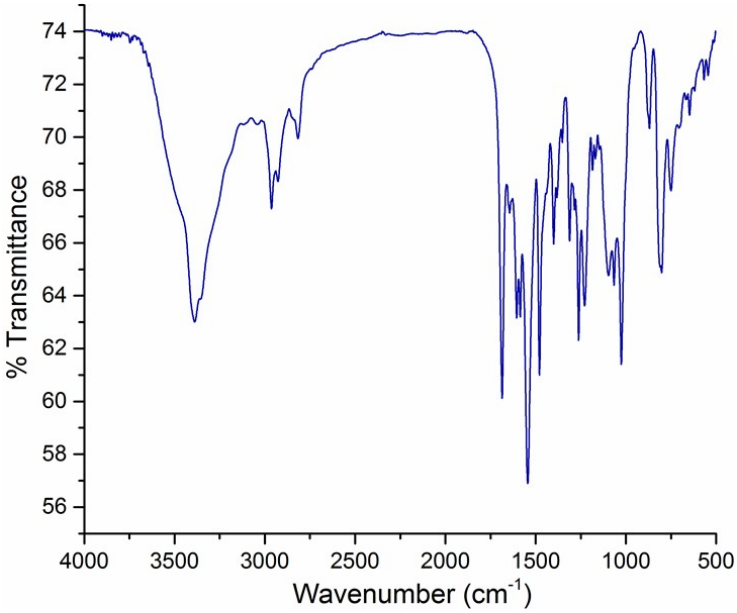

Figure S19: FT-IR spectrum of divalent hexafluorosilicate encapsulated complex **2c** of $\mathbf{L_2}$ recorded in KBr pellet.

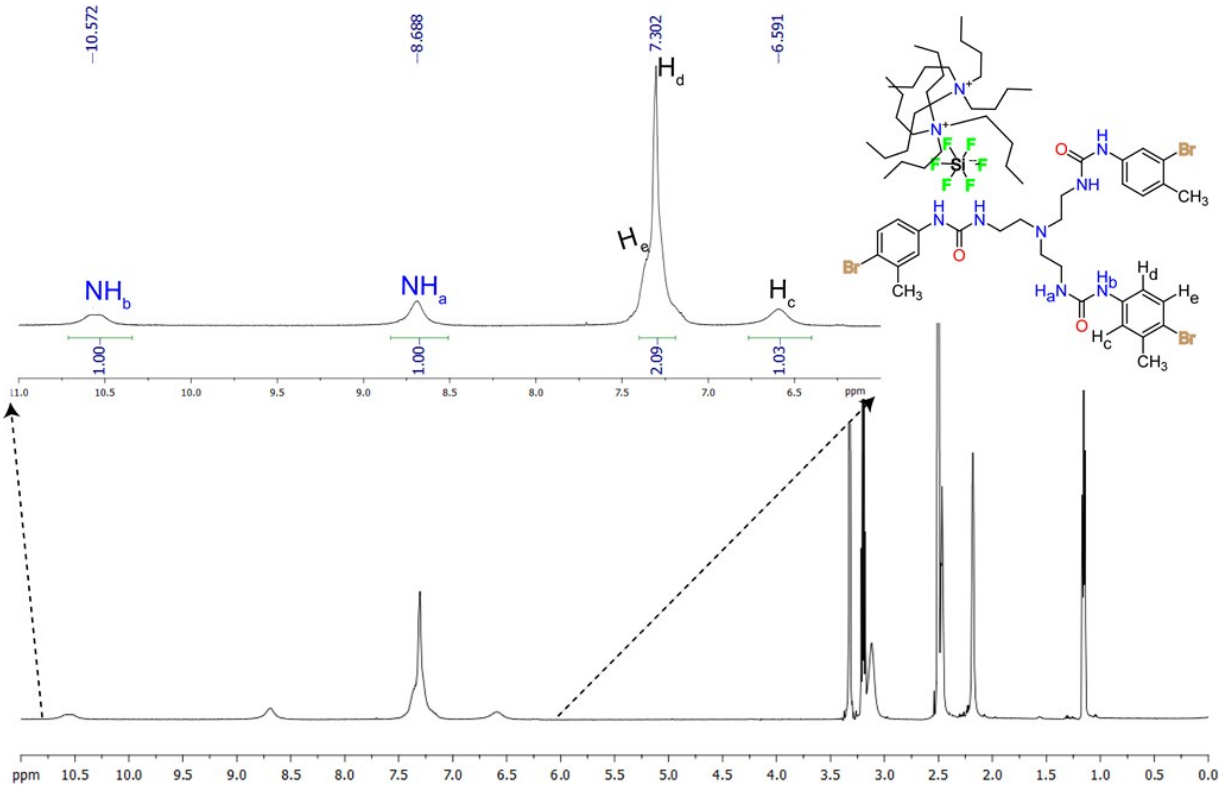

Figure S20: ^{1}H NMR full and expanded spectrum of divalent silicon hexafluoride encapsulated dimeric cage complex **2c** as recorded in DMSO-d_6 at 298 K.

Solution state anion binding studies:

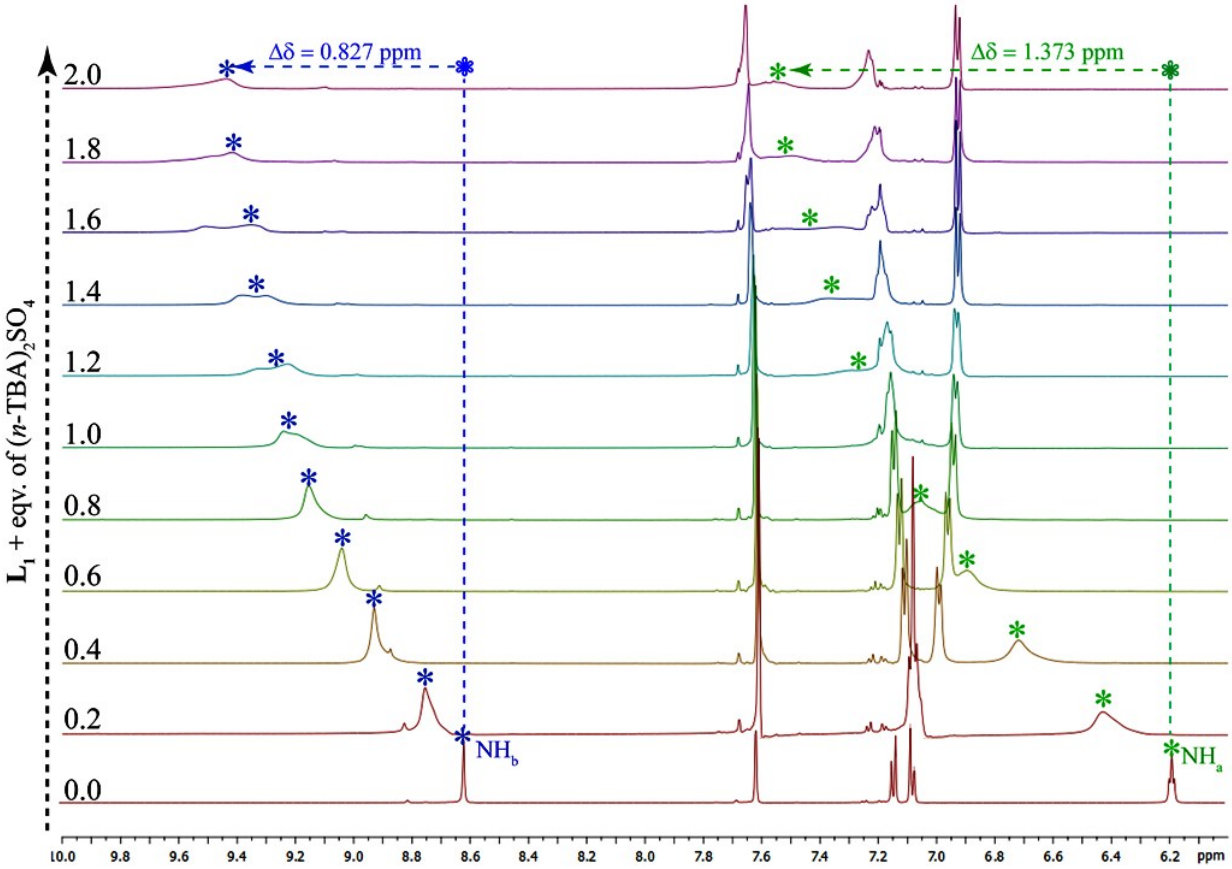

Figure S21: Expanded partial ^{1}H NMR stack plot of $\mathbf{L_1}$ upon titration with standard $(n\text{-TBA})_2SO_4$ in DMSO-d_6.

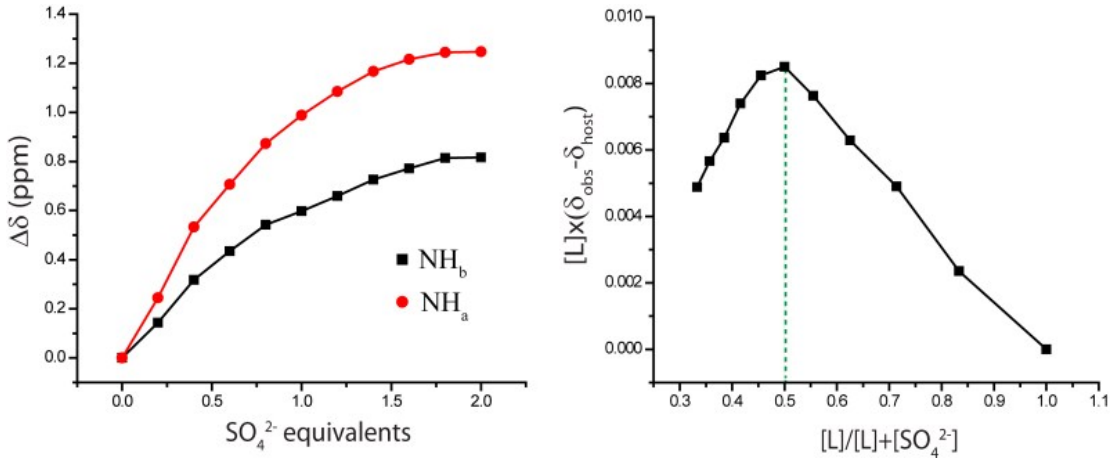

Figure S22: Change in chemical shift of –NH resonances of $\mathbf{L_1}$ (10 mM) with increasing concentration of standard SO_4^{2-} solution (50 mM) in DMSO-d_6 at 298 K and the corresponding Job's plot.

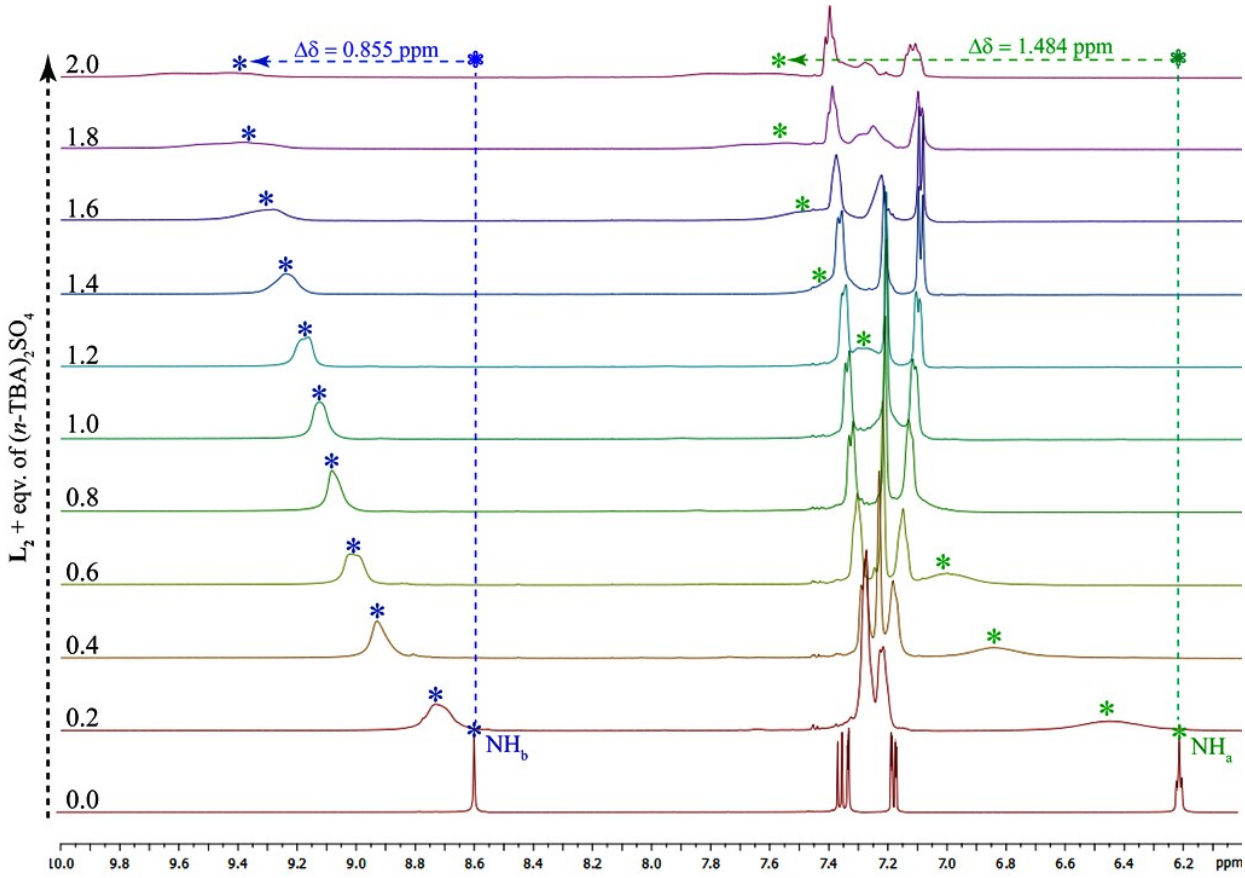

Figure S23: Expanded partial ^{1}H NMR stack plot of $\mathbf{L_2}$ upon titration with standard $(n\text{-TBA})_2SO_4$ in DMSO-d_6.

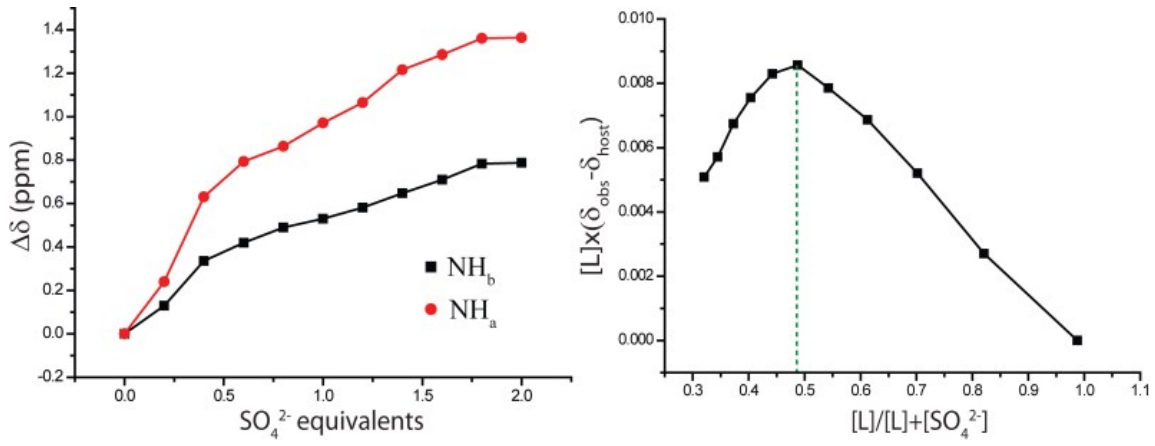

Figure S24: Change in chemical shift of –NH resonances of $\mathbf{L_2}$ (10 mM) with increasing concentration of standard SO_4^{2-} solution (50 mM) in DMSO-d_6 at 298 K and the corresponding Job's plot.

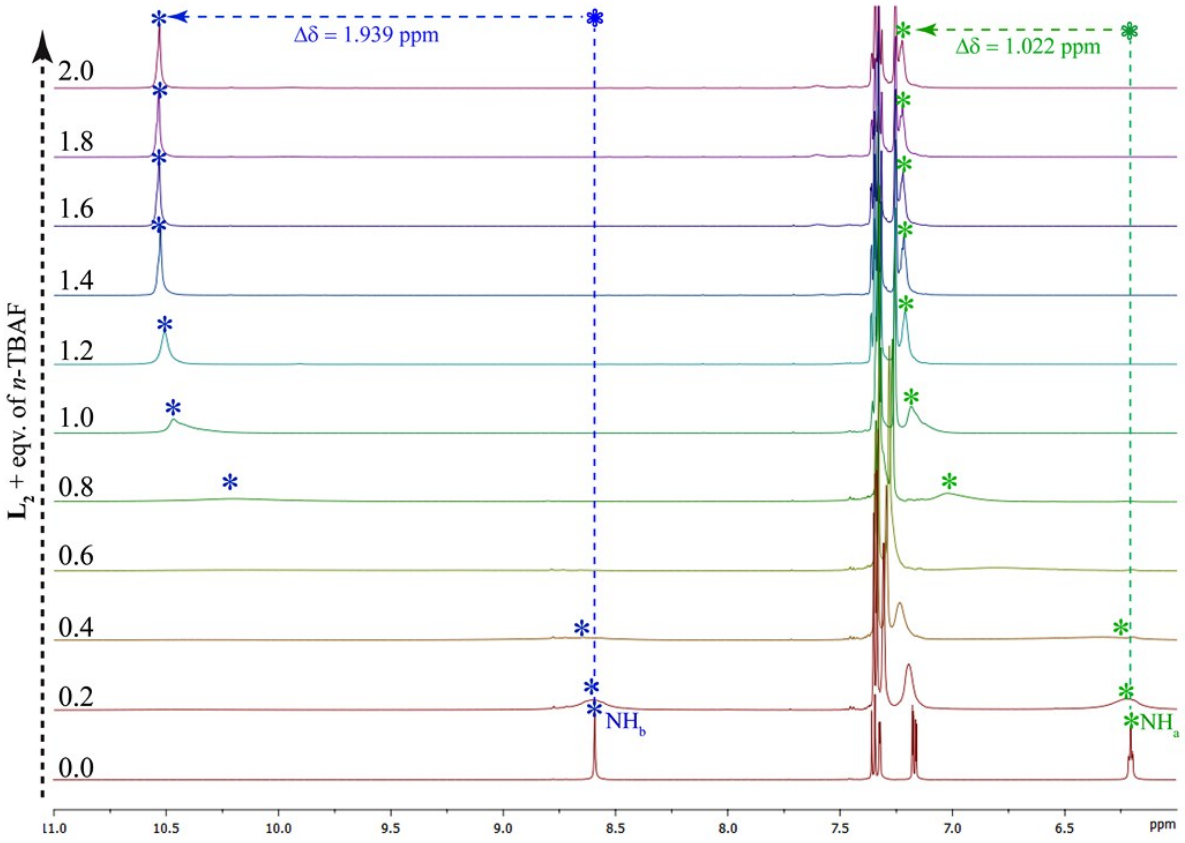

Figure S25: Expanded partial ^{1}H NMR stack plot of $\mathbf{L_2}$ upon titration with standard *n*-TBAF in DMSO-d_6 displaying instant downfield shift of urea –NH protons upon 1.0 eqv. fluoride salt addition.

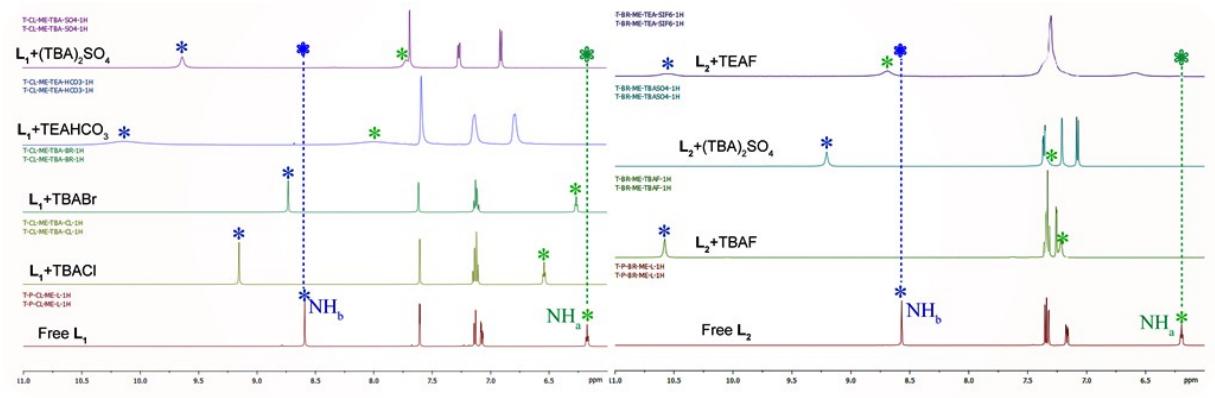

Figure S26. Expanded partial ^{1}H NMR comparative stacked spectra of receptors $\mathbf{L_1}$ (left) and $\mathbf{L_2}$ (right) with each anion as observed from the solid state, displaying the noticeable downfield shifts of urea -NH_a and -NH_b resonances of particular receptor upon anion complexation.

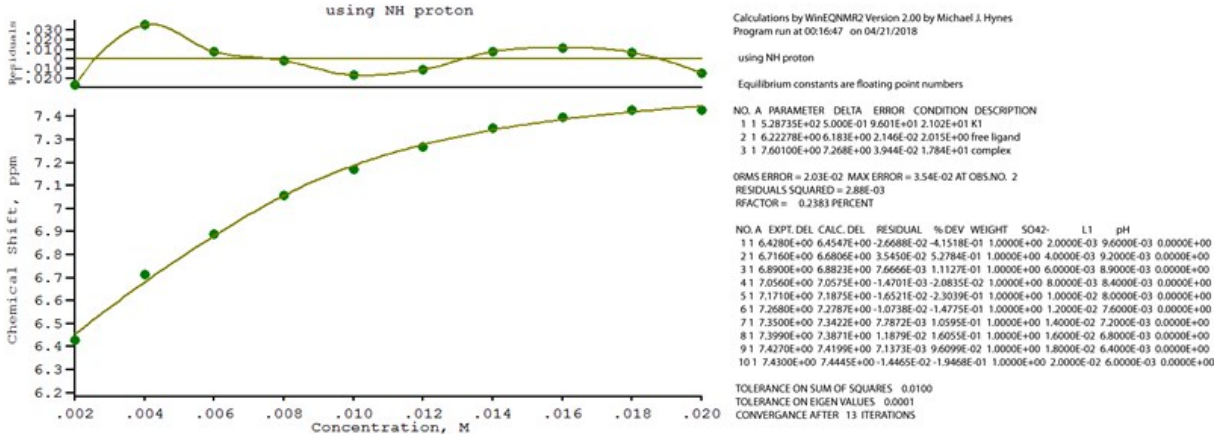

Figure S27: Change in chemical shift of $-NH_a$ resonances of $\mathbf{L_1}$ (10 mM) with increasing concentration of standard SO_4^{2-} solution (50 mM) in DMSO-d_6 (left) and the output files from WINEQNMR programme of $\mathbf{L_1}$-SO_4^{2-} titrations (right).

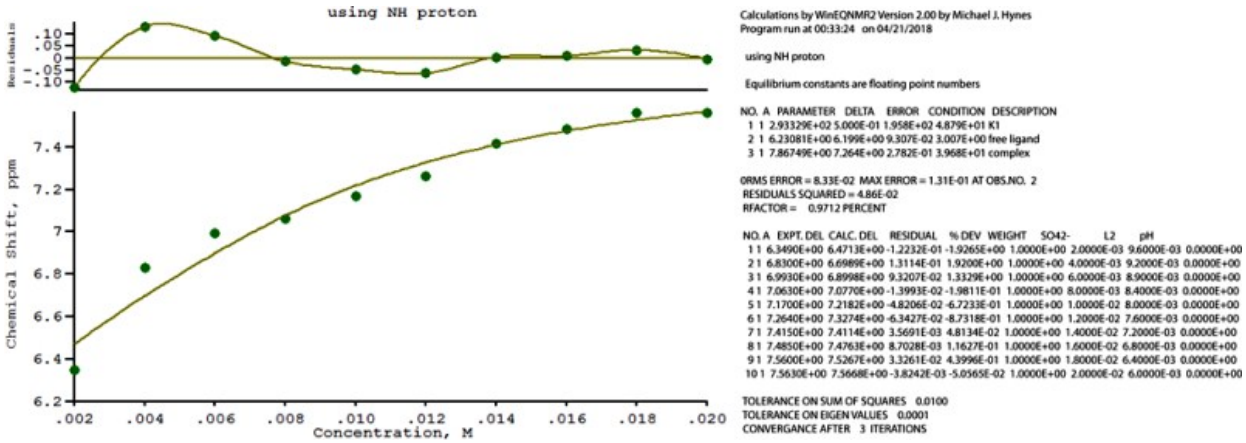

Figure S28: Change in chemical shift of $-NH_a$ resonances of $\mathbf{L_2}$ (10 mM) with increasing concentration of standard SO_4^{2-} solution (50 mM) in DMSO-d_6 (left) and the output files from WINEQNMR programme of $\mathbf{L_2}$-SO_4^{2-} titrations (right).

Table S1. Hydrogen bonding distances (Å) and Bond angles (°) in the free ligands and their anion complexes:

Complex	D–H···A	*d*(D···H)/Å	*d*(H···A)/Å	*d*(D···A)/Å	<D–H···A/°	Symmetry codes
L_1	N3-H3N···O2	0.86	1.99	2.847(10)	178	-x,-y,-z
	N4-H4N···O3	0.86	2.07	2.877(10)	157	x,y,z
	N5-H5N···O3	0.86	2.08	2.881(9)	155	x,y,z
	N6-H6N···O1	0.86	2.16	2.956(10)	154	1-x,-y,1-z
	N7-H7N···O1	0.86	2.13	2.921(9)	152	1-x,-y,1-z
L_2	N2-H2N···O3	0.86	2.13	2.927(9)	153	x,y,z
	N3-H3N···O3	0.86	2.12	2.907(9)	152	x,y,z
	N4-H4N···O4	0.86	2.19	2.971(9)	151	1+x,1/2-y,1/2+z
	N5-H5N···O4	0.86	2.11	2.899(8)	152	1+x,1/2-y,1/2+z
	N6-H6N···O6	0.86	2.01	2.869(9)	177	x,1/2-y,1/2+z
	N9-H9N···O5	0.86	2.12	2.919(8)	154	x,y,z
	N10-H10N···O5	0.86	2.20	2.991(8)	153	x,y,z
	N11-H11N···O2	0.86	2.01	2.870(9)	175	x,1/2-y,-1/2+z
	N13-H13N···O1	0.86	2.31	3.062(9)	147	x,1/2-y,-1/2+z
	N14-H14N···O1	0.86	2.01	2.827(9)	158	x,1/2-y,-1/2+z
1a	N2-H2N···Cl4	0.86	2.66	3.449(12)	154	-1/2+x,1/2-y,z
	N3-H3N···Cl4	0.86	2.49	3.301(11)	158	-1/2+x,1/2-y,z
	N4-H4N···Cl4	0.86	2.65	3.443(12)	153	-1/2+x,1/2-y,z
	N5-H5N···Cl4	0.86	2.43	3.274(8)	166	-1/2+x,1/2-y,z
	N6-H6N···Cl4	0.86	2.74	3.527(9)	153	-1/2+x,1/2-y,z
	N7-H7N···Cl4	0.86	2.39	3.220(13)	162	-1/2+x,1/2-y,z
1b	N2-H2N···Br1	0.86	2.77	3.5595	153	-1/2+x,1/2-y,z
	N3-H3N···Br1	0.86	2.50	3.3416	166	-1/2+x,1/2-y,z
	N4-H4N···Br1	0.86	2.85	3.6309	152	-1/2+x,1/2-y,z
	N5-H5N···Br1	0.86	2.52	3.3233	156	-1/2+x,1/2-y,z
	N6-H6N···Br1	0.86	2.77	3.5670	154	-1/2+x,1/2-y,z
	N7-H7N···Br1	0.86	2.61	3.4295	159	-1/2+x,1/2-y,z
1c	N2-H2N···O8	0.86	2.19	2.975(10)	151	x,y,z
	N3-H3N··· O8	0.86	2.13	2.920(10)	153	x,y,z
	N4-H4N···O7	0.86	2.17	2.884(12)	141	1/2-x,y,3/2-z
	N5-H5N···O7	0.86	2.41	3.075(13)	134	1/2-x,y,3/2-z
	N5-H5N···O8	0.86	2.36	3.201(10)	166	1/2-x,y,3/2-z
	N6-H6N···O8	0.86	2.31	3.152(10)	167	x,y,z
	N7-H7N···O7	0.86	1.89	2.748(13)	173	x,y,z
	N7-H7N···O7	0.86	2.35	3.094(14)	144	1/2-x,y,3/2-z
	N9-H9N···O10	0.86	2.50	3.239(8)	144	x,y,z
	N10-H10N···O10	0.86	2.08	2.868(12)	153	x,y,z
	N11-H11N···O9	0.86	2.44	3.160(10)	141	x,y,z
	N12-H12N···O9	0.86	2.14	2.984(12)	167	1/2-x,y,1/2-z
	N13-H13N···O9	0.86	2.52	3.253(10)	144	x,y,z

	N14-H14N···O9	0.86	1.93	2.792(10)	175	x,y,z
1d	N2-H2N···O7	0.86	2.12	2.937(5)	160	x,y,z
	N3-H3N···O9	0.86	2.19	3.018(5)	161	x,y,z
	N4-H4N···O7	0.86	2.12	2.904(6)	152	x,y,z
	N5-H5N···O8	0.86	2.12	2.941(5)	158	x,y,z
	N6-H6N···O7	0.86	2.08	2.908(5)	160	x,y,z
	N7-H7N···O10	0.86	2.13	2.951(5)	159	x,y,z
	N9-H9N···O9	0.86	2.24	3.025(5)	152	x,y,z
	N10-H10N···O9	0.86	2.08	2.915(6)	164	x,y,z
	N11-H11N···O8	0.86	2.24	3.028(5)	152	x,y,z
	N12-H12N···O8	0.86	2.10	2.932(5)	161	x,y,z
	N13-H13N···O10	0.86	2.30	3.077(5)	150	x,y,z
	N14-H14N···O10	0.86	1.10	2.931(5)	163	x,y,z
2a	N2-H2N···F1	0.86	2.03	2.826(6)	154	x,y,z
	N3-H3N··· F1	0.86	2.01	2.816(6)	156	x,y,z
	N4-H4N··· F1	0.86	2.29	3.033(5)	144	x,y,z
	N5-H5N··· F1	0.86	1.88	2.721(6)	164	x,y,z
	N6-H6N··· F1	0.86	2.24	2.982(5)	144	x,y,z
	N7-H7N··· F1	0.86	1.90	2.720(6)	160	x,y,z
2b	N2-H2N···O7	0.86	2.36	3.134(14)	150	x,y,z
	N3-H3N···O7	0.86	2.06	2.908(17)	167	x,y,z
	N4-H4N···O9	0.86	2.33	3.109(16)	151	x,y,z
	N5-H5N···O9	0.86	2.11	2.947(16)	165	x,y,z
	N6-H6N···O10	0.86	2.21	3.006(14)	154	x,y,z
	N7-H7N···O10	0.86	2.30	3.054(14)	146	x,y,z
	N9-H9N···O8	0.86	2.14	2.897(15)	146	x,y,z
	N10-H10N···O7	0.86	2.11	2.945(16)	165	x,y,z
	N11-H11N···O8	0.86	2.14	2.910(13)	148	x,y,z
	N12-H12N···O9	0.86	2.26	3.077(16)	159	x,y,z
	N13-H13N···O8	0.86	2.19	2.957(16)	149	x,y,z
	N14-H14N···O10	0.86	2.11	2.943(15)	163	x,y,z
2c	N2-H2N···F1	0.86	1.97	2.800(3)	161	x,y,z
	N3-H3N··· F4	0.86	2.46	3.220(2)	148	x,y,z
	N4-H4N··· F1	0.86	2.41	3.155(18)	145	x,y,z
	N5-H5N··· F3	0.86	2.27	3.100(2)	161	x,y,z
	N6-H6N··· F1	0.86	2.16	2.933(19)	150	x,y,z
	N7-H7N··· F2	0.86	2.17	3.000(2)	164	1-x,y,1/2-z

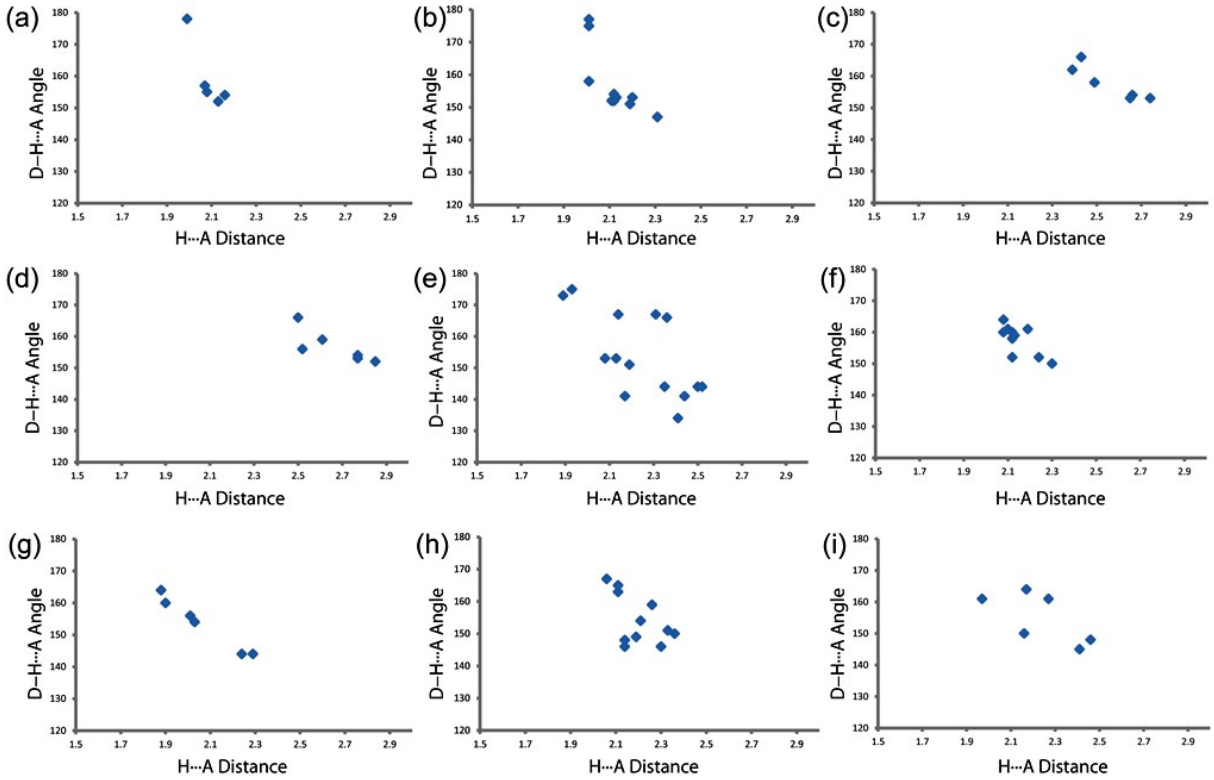

Figure S29. The scatter plot of D–H···A angles *vs*. H···A distances of the hydrogen bonds in free receptors (a) $\mathbf{L_1}$, (b) $\mathbf{L_2}$ and in their neutral anion complexes (c) **1a**, (d) **1b**, (e) **1c**, (f) **1d**, (g) **2a**, (h) **2b** and (i) **2c**.